Proceedings of the 29th Annual International
Conference of the IEEE EMBS
Cité Internationale, Lyon, France
August 23-26, 2007.

A Medical Texture Local Binary Pattern For TRUS Prostate Segmentation

Nezamoddin N. Kachouie and Paul Fieguth
Department of Systems Design Engineering
University of Waterloo, 200 University Ave. West, Waterloo, Ontario, Canada

Abstract— **Prostate cancer diagnosis and treatment rely on segmentation of Transrectal Ultrasound (TRUS) prostate images. This is a challenging and difficult task dut to weak prostate boundaries, speckle noise and the short range of gray levels. Advances in digital imaging techniques have made it possible the acquisition of large volumes of TRUS prostate images so that there is considerable demand for automated segmentation systems.**

Local Binary Pattern (LBP) has been used for texture segmentation and analysis. Despite its promising performance for texture classification it has not yet been considered for TRUS prostate segmentation. In this paper we introduce a medical texture local binary pattern operator designed for applications of medical imaging where different tissues or micro organisms might maintain extremely weak underlying textures that make it impossible or very difficult for ordinary texture analysis approaches to classify them. In the proposed method the deformations of a level set contour are controlled based on the medical texture local binary pattern operator.

I. INTRODUCTION

As the most diagnosed cancer, prostate cancer is the second leading cause of the cancer death in North America [1]. Hence diagnosis of the cancer in the early stages is crucial. Prostate TRUS images in comparison with the other modalities such as CT and MRI are captured easier, in real-time, and with lower cost so they are widely used for diagnosis of prostate cancer, cancer treatment planing, needle biopsy, and brachytherapy.

The size and the shape of the prostate must be extracted by prostate segmentation to diagnose the cancer stage. Although experts can infer these information manually from TRUS prostate images in the traditional method, the manual method is tedious, expensive, time consuming, and subjective. Given the increasing amount of TRUS images being collected, automated methods of TRUS prostate segmentation are in high demand and different segmentation methods have been proposed. These methods include region segmentation methods, boundary segmentation techniques, and deformable models [2], [3], [4], [5], [6], [7], [8], [9]. Prostate region in TRUS prostate images maintains very weak texture structure. Because of the speckle noise, short range of gray levels, very weak prostate region texture, and shadow regions the ordinary texture analysis methods are not capable to capture, discriminate, and segment the prostate region based on its texture. There have been some attempts by employing the Gabor filter bank for prostate texture segmentation [10], [5], however prostate texture analysis has not yet been investigated seriously. We introduce a novel method by specializing Local Binary Pattern (LBP) for texture analysis of medical images. In this paper the proposed method is adapted specifically for TRUS prostate image segmentation to capture the prostate texture.

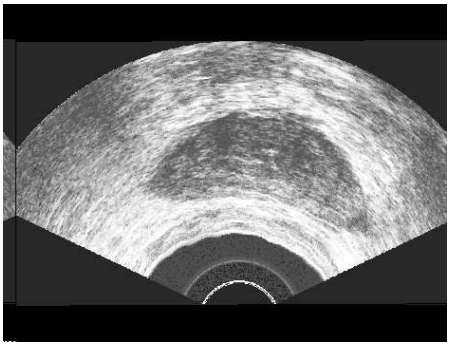

Fig. 1. Original TRUS prostate image.

II. LOCAL BINARY PATTERN (LBP)

The local binary pattern (LBP) operator was introduced by Ojala et al. [11] in 1996 as a measure of local image contrast. Since then it has been employed for different applications of texture classification [12], [13]. A typical $n \times n$ neighbourhood for $n = 3$ is depicted in Tab. I(left). The centre pixel value I_i^0 of the neighbourhood is considered as a threshold. Threshold function T is defined based on the

I_i^1	I_i^2	I_i^3
I_i^8	I_i^0	I_i^4
I_i^7	I_i^6	I_i^5

1	2	4
128		8
64	32	16

lbp_i^1	lbp_i^2	lbp_i^3
lbp_i^8		lbp_i^4
lbp_i^7	lbp_i^6	lbp_i^5

TABLE I

LEFT: AN EXAMPLE 3×3 WINDOW. MIDDLE: WEIGHTING MAP. RIGHT: WEIGHTED THRESHOLDED VALUES.

This research has been funded by the Natural Science and Engineering Research Council of Canada (NSERC).

We would like to thank Mr. Shahryar Rahnamayan for providing TRUS prostate images for this research.

23	29	7
25	16	5
16	14	21

1	1	0
1		0
1	0	1

1	2	0
128		0
64	0	16

67	70	64
62	16	73
59	57	63

1	1	1
1		1
1	1	1

1	2	4
128		8
64	32	16

TABLE II

LEFT: EXAMPLE WINDOWS. MIDDLE: THRESHOLDED VALUES. RIGHT: WEIGHTED THRESHOLDED VALUES.

23	29	7
25	16	5
16	14	21

1	1	1
1		1
1	1	1

1	2	4
128		8
64	32	16

67	70	64
62	16	73
59	57	63

0	0	0
0		0
0	0	0

0	0	0
0		0
0	0	0

TABLE III

LEFT: EXAMPLE WINDOWS. MIDDLE: THRESHOLDED VALUES. RIGHT: WEIGHTED THRESHOLDED VALUES.

differences of the central pixel and its neighbours as

$$T(I_i^j, I_i^0) = \begin{cases} 1 & \text{if } I_i^j - I_i^0 \geq 0 \\ 0 & \text{Otherwise.} \end{cases} \quad (1)$$

where $j \in [1, n^2 - 1]$ and I_i^j is the value of j^{th} neighbouring pixel of the central pixel i. A $n \times n$ weighting map corresponding to the neighbouring pixels is considered to be multiplied by thresholded values. A weighting map is depicted in Tab. I(middle). As it can be seen in Tab. I(right), the LBP of I_i^0 can be computed by summing up the weighted thresholded values:

$$LBP = \sum_{j=1}^{8} lbp_i^j \quad (2)$$

where,

$$lbp_i^j = T(I_i^j, I_i^0) \times w_i^j \quad (3)$$

Two example 3×3 windows are depicted in Tab. II(left). In the both examples the central pixel is 16. The centre pixel in the top row belongs to a smooth region while it is an outlier in the bottom row. Associated LBP is 211 for the top row and 255 for the botoom one. As we can observe completely different cases result in very close values of LBP.

III. THE PROPOSED METHOD

Although different organs, tissues, and cellular structures have often their specific textures, the corrsponding underlying textures are very weak so that they cannot be captured by ordinary texture analysis methods.

LBP is a strong texture discriminator operator. It can potentially be applied to medical/biomedical image analysis, however in its general form it cannot be effectively employed for texture analysis applications in this area.

A. Medical Texture LBP (MTLBP)

We propose a specialized medical texture local binary pattern (MTLBP) in this paper for medical texture analysis which is specifically adapted for TRUS prostate image segmentation. The proposed MTLBP is

$$MTLBP = \begin{cases} \sum_{i=1}^{8} D(I_i^j, I_i^0) \times w_i^j & \text{if } I_i^0 \in [g_1, g_2] \\ 0 & \text{Otherwise.} \end{cases} \quad (4)$$

where, g_1 and g_2 are lower and upper bound of the values of the texture and D is a discriminant function and is defined based on the probability density function of the textured region. Two cases are considered for the PDF as follows.

A single Gaussian represents the PDF of the texture:

$$D(I_i^j, I_i^0) = \begin{cases} 1 & \text{if } I_i^j \in [g_1, g_2] \\ 0 & \text{Otherwise.} \end{cases} \quad (5)$$

A Gaussian mixture represents the PDF of the texture:

$$D(I_i^j, I_i^0) = \begin{cases} 1 & \text{if } I_i^j \in [g_1, g_2] \ \& \ |I_i^0 - I_i^j| \leq T_k \\ 0 & \text{Otherwise.} \end{cases} \quad (6)$$

where, T_k is upper bound of k^{th} Gaussian of the mixture:

$$T_k = \mu_k + \lambda \cdot \sigma_k \quad (7)$$

where, μ_k, λ_k, and σ_k are the mean, a constant and the standard deviation of the k^{th} Gaussian of the mixture. The associated MTLBP for the same examples as the previous section are depicted in Tab. III where the texture is assumed as a single Gaussian and $[g1, g2] = [0, 40]$. As we can observe the associated MTLBP to the top row where we have a smooth region is 255 while it is zero for the bottom row where the central pixel is an outlier. Although LBP associates very close values to both examples, MTLBP clearly discriminates them to two different classes.

B. Gradient of MTLBP

In the first step we apply the proposed MTLBP to the TRUS prostate images. Fig. 2(a) shows the resultant image after applying MTLBP to the Fig. 1. To further discriminate the prostate region, an equidistant boundary separating foreground and background is illustrated by computing the distance of the foreground pixels from the background and obtaining the gradient of the resultant image. Figs. 2(b), (c) and (d) show the horizontal, vertical, and magnitude of the gradient image respectively.

The magnitude of gradient will be thresholded by a threshold T_{mag} that minimizes the inter-class variance. Morphology operators are eventually applied to emphasize the

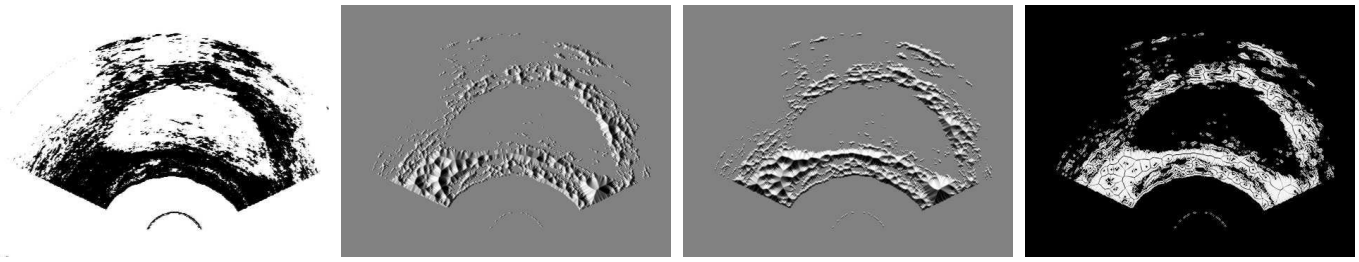

(a) (b) (c) (d)

Fig. 2. (a) MTLBP associated to the Fig. 1. Gradient of equidistant boundary of MTLBP: (b) In the X-Direction. (c) In the Y-Direction. (d) Its magnitude.

prostate edges. A linear mask with 45° and 135° orientations is dilated over the thresholded gradient image.

$$G \oplus M \equiv \{G_i + M_j : G_i \in G,\ M_j \in M\} = \bigcup_{M_j \in M} G_{+M_j} \tag{8}$$

where G is the gradient of MTLBP, M is the mask and

$$G_{+M_j} \equiv \{G_i + M_j :\ G_i \in G\} \tag{9}$$

is the translation of G along the M_j. Figs. 3(a) and (b) show the thresholded magnitude image and the dilated result respectively.

C. Level Set

A level set contour will deform toward prostate boundary in the last step. The dilated gradient MTLBP image is the external force that controls the deformations of the zero level set contour toward the prostate boundary.

An elliptical contour, the zero level set of a $3-D$ hyper ellipse, is considered as

$$\frac{(x-c_x)^2}{a^2} - \frac{(y-c_y)^2}{b^2} = 1 \tag{10}$$

where (a,b) are the ellipse horizontal and vertical axis and (c_x, c_y) are the ellipse center coordinates. Having the zero level set initialized as an elliptical contour, velocity function F is designed based on the gradient image so that the interface evolves toward the prostate boundary and converges in its vicinity.

$$F = -exp\{\epsilon\aleph - \alpha V_g\} \tag{11}$$

where $\aleph$ and ϵ are curvature and curvature coefficient respectively, and V_g and α are gradient based velocity and its constant coefficient. The dilated gradient MTLBP, G, represents the gradient based velocity, i.e., $V_g = G$ and

$$\aleph = \nabla.\frac{\nabla\Phi}{|\nabla\Phi|} = \left\{\frac{\Phi_{xx}\Phi_y^2 - 2\Phi_x\Phi_y\Phi_{xy} + \Phi_{yy}\Phi_x^2}{(\Phi_x^2+\Phi_y^2)^{\frac{3}{2}}}\right\} \tag{12}$$

IV. Results

Assuming $g_1 = 0$, $g_2 = 40$, and a single Gaussian representing the prostate texture, the proposed MTLBP is applied to the TRUS prostate images to derive the results. The original image is depicted in Fig. 1 while the associated MTLBP image is depicted in 2(a). MTLBP image is then employed to design the proper velocity function that will control the level set contour deformations toward the prostate boundary.

The foreground-background distance is computed to find the equidistant boundary separating prostate region from the background. As it can be observed in Fig. 2 the gradient of the resultant equidistant boundary almost clearly separates the prostate from the background. Gradient in the X-Direction, Y-Direction, and its magnitude are depicted in Fig. 2.

To emphasize the edges we threshold the gradient image by minimizing the inter-class variance and dilate the result by a linear mask with 45° and 135° orientations. The thresholded image and the dilated one are depicted in Fig. 3. Finally an elliptical contour initializes the zero level set of a $3-D$ deformable hyper-interface which its deformations are controlled by dilated gradient MTLBP as the external force. The initial elliptical interface and its deformations toward prostate boundary are depicted in Figs. 3(c) and 4 respectively. The preliminary results are promising and as it can be observed, the proposed MTLBP method is able to successfully segment the prostate boundary in TRUS images.

V. Conclusions and Discussions

Prostate texture analysis is a very difficult and challenging task due to weak prostate texture structure, the speckle noise, and shadow regions. Hence the ordinary texture analysis methods are not capable of capturing and discriminating the prostate region based on its texture. In this paper we introduced a novel method by specializing Local Binary Pattern for medical texture analysis. The proposed Medical Texture Local Binary Pattern has strong discriminative attributes that can be effectively used for texture classification. In this paper the proposed method is adapted specifically for TRUS prostate image segmentation to capture the prostate texture. As the preliminary results are quite promising, our future work focuses on applications of the proposed MTLBP for multi texture analysis of medical images.

References

[1] "Cancer facts and figures, http://www.cancer.org," *Amr. Cancer society*.

[2] C.K. Kwoh, M. Teo, W. Ng, S. Tan, and M. Jones, "Outlining the prostate boundary using the harmonics method," *Med. Biol. Eng. Computing*, vol. 36, pp. 768–771, 1998.

(a) (b) (c)

Fig. 3. (a) Thresholded gradient of MTLBP by minimizing the inter-class variance. (b) Dilated thresholded image obtained by applying a linear mask with 45° and 135° orientations to the thresholded gradient. (c) Elliptical initialization of the level set.

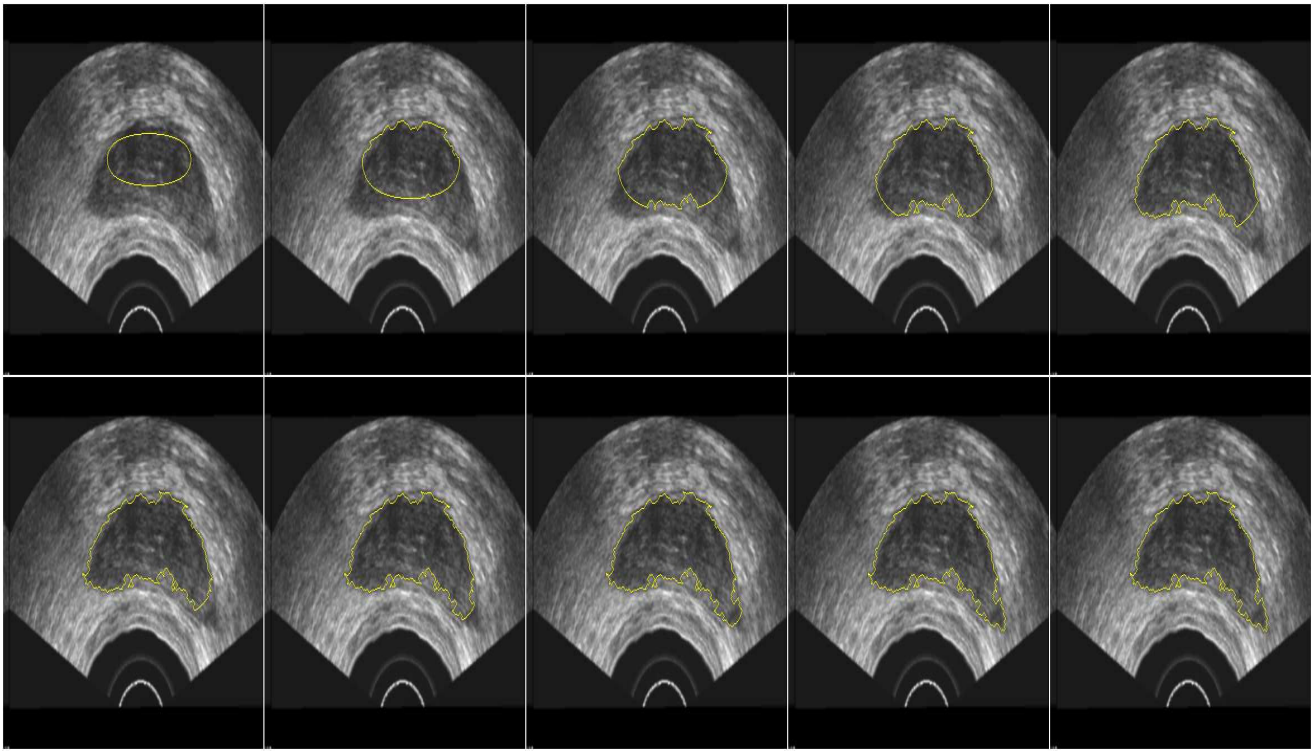

Fig. 4. The deformations of the level set for 250 iterations where the contour converges and stops in the vicinity of the prostate boundary. Frames are departed by 25 iterations.

[3] R.G. Aarnink, R.J.B. Giesen, A. L. Huynen, J. J. de la Rosette, F.M. Debruyne, and H. Wijkstra, "A practical clinical method for contour determination in ultrasound prostate images," *Ultrasound Med. Biol.*, vol. 20, pp. 705–717, 1994.

[4] R.G. Aarnink, S.D. Pathak, J. J. de la Rosette, F.M. Debruyne, Y. Kim, and H. Wijkstra, "Edge detection in ultrasound prostate images using integrated edge map.," *Ultrasound Med. Biol.*, vol. 36, pp. 635–642, 1998.

[5] Y. Zhan and D. Shen, "Deformable segmentation of 3-d ultrasound prostate images using statistical texture matching method," *IEEE Transactions on Medical Imaging*, vol. 25, pp. 256–272, 2006.

[6] D. Freedman, R.J. Radke, T. Zhang, Y. Jeong, D.M. Lovelock, and G.T.Y. Chen, "Model-based segmentation of medical imagery by matching distributions," *IEEE Transactions on Medical Imaging*, vol. 24, pp. 281–292, 2005.

[7] A. Ghanei, H. Soltanian-Zadeh, A. Ratkewicz, and F. Yin, "A three dimentional deformable model for segmentation of human prostate from ultrasound images," *Med. Phys*, vol. 28, pp. 2147–2153, 2001.

[8] C. Knoll, M. Alcaniz, V. Grau, C. Monserrat, and M. Juan, "Outlining of the prostate using snakes with shape restrictions based on the wavelet transform," *Pattern Recognition*, vol. 32, pp. 1767–1781, 1999.

[9] S. D. Pathak, V. Chalana, D. haynor, and Y. kim, "Edge guided boundary delineation in prostate ultrasound images," *IEEE Transactions on Medical Imaging*, vol. 19, pp. 1211–1219, 2000.

[10] S. S. Mohamed, T. K. Abdel-galil, M. M. Salma, A. Fenster, D. B. Downey, and K. Rizkalla, "Prostate cancer diagnosis based on gabor filter texture segmentation of ultrasound image," *IEEE CCECE*, vol. , pp. 1485–1488, 2003.

[11] T. Ojala, M. Pietikinen, and D. Harwood, "A comparative study of texture measures with classification based on featured distribution," *Pattern Recognition*, vol. 29, pp. 51–59, 1996.

[12] P. Wang, SM. Krishnan, C. Kugean, and MP. Tjoa, "Classification of endoscopic images based on texture and neural network," in *23rd Annual EMBS International Conference*, 2001, pp. 3691–3695.

[13] K. Caballero, J. Barajas, O. Pujol, N. Savatella, and P. Radeva, "In-vivo ivus tissue classification: a comparison between rf signal analysis and reconstructed images," *Lecture Notes in Computer Science: 11th Iberoamerican Congress in Pattern Recognition*, vol. 4225, pp. 137–146, 2006.